Coordinated Control of an HVDC Link and Doubly Fed Induction Generators in a Large Offshore Wind Farm

Dawei Xiang, Li Ran, *Member, IEEE*, Jim R. Bumby, Peter J. Tavner, and Shunchang Yang

***Abstract*—Doubly fed induction generators (DFIGs) are an economic variable-speed solution for large wind turbines while high-voltage dc (HVdc) transmission is being considered for the grid connection of some offshore wind farms. This paper analyzes the need for coordinating the control of the DFIGs and the HVdc link so that the two topologies can work together, giving system designers and operators a choice that may be useful in some applications. It is desired that individual generators be controlled for power tracking in a way similar to that used when they are connected directly to an ac grid, although a grid voltage reference for the DFIG control is no longer available as an independent source in this case. The study shows that machine control should explicitly maintain the flux level, which then allows the HVdc link to regulate the local system frequency and, indirectly, voltage amplitude. Interactions between DFIGs and the HVdc link are investigated and simulations performed to verify the proposed control strategy.**

***Index Terms*—Doubly fed induction generator, frequency, high-voltage dc (HVdc) transmission, real and reactive power, voltage, wind energy.**

I. Introduction

WIND TURBINES are arguably the most developed source of renewable electrical energy with ratings of commercial wind turbines now exceeding 4 MW. Attractive locations for future large turbines would be remote, such as offshore, where wind conditions are improved and planning restrictions are reduced. Variable speed is essential for large turbines partially because this attenuates the mechanical stresses that the turbine blades and towers are subject to [1]. There have been active studies regarding the topologies of variable-speed turbines including those using cage induction [2] and slow rotating, direct-drive machines [3]. Such topologies usually require 100% rated, four-quadrant power-electronic converters. As the converter cost decreases, such topologies will no doubt become increasingly more popular. In contrast, a traditional solution has been the doubly fed induction generator (DFIG) which typically requires a 25% rated, 4-quadrant converter between the rotor and grid for the speed range needed. As a result, the DFIG has been an economic solution for large, variable-speed wind turbines despite its disadvantages of having a wound rotor and a brush-slip ring arrangement.

DFIGs are usually connected to the ac mains on the stator side. Existing DFIG wind turbines are all located with ac mains easily available. As the wind industry develops, there is interest in building larger wind farms further offshore (e.g., off northwest Great Britain). Several wind farms are planned to be built beyond offshore islands and are expected to have registered capacities around 1000 MW with distances of more than 100 km to the nearest grid connection point. If high-voltage subsea cables are to be used for ac interconnection, the charging reactive power associated with the cable capacitance will be significant. For instance, the total charging power of a three-phase, 400-kV cable will be above 1500 MVAr, assuming a distance of 100 km [4], which cannot be easily handled by the DFIGs using the rotor side control. Therefore, it may be necessary to use dc interconnection. Previous studies have considered the advantages of using voltage-source converter (VSC)-based dc links when the transmitted power and transmission distance justify the choice [2], [5], [6]. Regarding the power level concerned in the present study, this paper will focus on the thyristor-based HVdc link which, given the present conditions of technology, could achieve the desired high voltage at relatively low cost. DFIGs are still considered a valid option for large turbines as the speed of each turbine can be independently varied.

It seems that some redundancy has been caused between the power-electronic conversion stages in the DFIGs and the HVdc link. However, the DFIG pulse-width-modulated (PWM) converter is used to adjust the turbine speed and for power tracking while thyristor bridges in the HVdc link are for ac-dc conversion and for the power transmission purpose. If cage induction machines are used instead of DFIGs, the turbines will not be able to vary the power capture as the wind speed changes and turbines will all run at virtually the same speed. Furthermore, compensators, such as STATCOM, are needed to provide the reactive power. Similarly, wind turbines using synchronous machines will also prevent the speed of individual turbines being independently controlled. Machine-side power-electronic conversion is always necessary for variable-speed turbines. Although some proposed topologies, such as that described in [2], can integrate the power conversion stages for machine control and high-voltage dc transmission, issues including machine-to-ground insulation and/or large scale dc-dc voltage transformation, need to be further addressed. It is in this circumstance that the DFIG plus HVdc topology is considered a candidate in several anticipated

Manuscript received October 27, 2004; revised March 15, 2005. This work was supported by the New and Renewable Energy Centre (NaREC), Blyth, U.K. Paper no. TPWRD-00505-2004.

D. Xiang and S. Yang are with the Department of Electrical Engineering, Chongqing University, Chongqing 400044, China.

L. Ran, J. R. Bumby, and P. J. Tavner are with the School of Engineering, Science Laboratories, University of Durham, Durham DH1 3LE, U.K. (e-mail: li.ran@durham.ac.uk).

Digital Object Identifier 10.1109/TPWRD.2005.858785

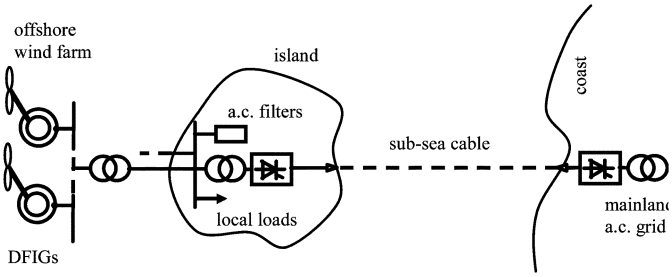

Fig. 1. System configuration.

applications in the near future. Further discussion on possible topologies in similar cases can be found in [7].

Given speed, rotor voltage, and frequency of a DFIG, we can specify the voltage and frequency on the stator side. This is, however, not the case in DFIGs for wind turbines in which a torque-speed characteristic should be defined for maximum power tracking [8]. Operating an HVdc link with a wind farm of DFIGs is thus challenging and no previous knowledge is available for the topology. The HVdc link cannot define an independent ac voltage reference for the DFIG to control its power. This is also a new situation from the HVdc system point of view. For the reasons to be expanded later, the HVdc link is responsible for maintaining the local system frequency. But this is not achieved by affecting the balance of mechanical and electrical power on the machines as the electrical power would already be subject to individual DFIG control for power tracking. The success of an integrated DFIG and HVDC system will rely on an in-depth understanding of the interactions between the two technologies. This study investigates such complex interactions and proposes a control strategy based on the knowledge obtained. It is hoped that the study will broaden the choices of system designers and future operators when considering a link for a large, offshore wind farm to the grid requiring long subsea cables.

II. Control Principles

Fig. 1 shows the configuration of the studied system. An offshore wind farm is connected to the mainland grid using an HVdc link. An island provides space for the rectifier station; some local loads on the island need to be supplied from the wind farm. Parameters of such a system, used to illustrate the interactions involved, will be described later in the paper.

According to the operating principle of a DFIG in the wind turbine context, it is generally possible to set its output real and reactive power at a practical stator frequency and rotor speed. This is achieved by vector control implemented in the rotor-side converter [9], [10]. The output real power is varied to follow the variation of wind speed. A preset cubic relationship between the generator output power and the rotor speed is embedded in the control algorithm. In the steady-state, the total real power generated by all DFIGs must balance the power taken away by the HVdc link plus the local loads and losses. Similarly, the balance of reactive power must also be maintained. Unbalance of real and reactive power during a transient may cause variations of the frequency and voltage in the local ac system. This is to be investigated to allow the HVdc link to regulate the frequency and voltage.

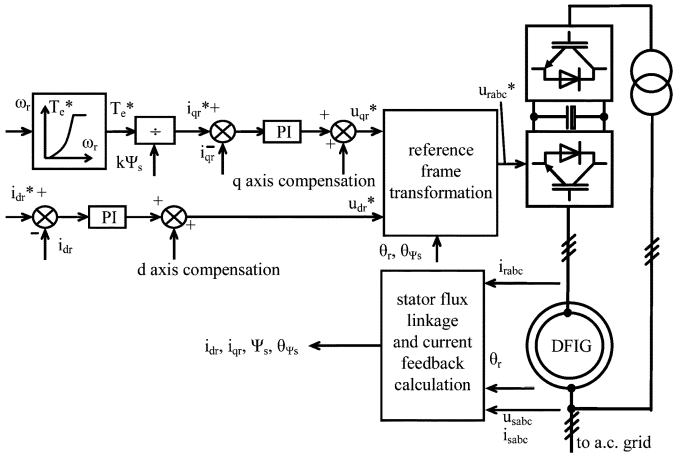

Fig. 2. Controller of a grid-connected DFIG.

This section describes the control principles of the DFIGs and HVdc link and considers from a theoretical point of view, the interaction between the two parts of the system.

A. Control of DFIG

The basic idea of vector control for a DFIG is to specify the reactive power and air-gap torque of the machine through two orthogonal components of the rotor current in a defined reference frame. This is similar to the vector control of induction motor drives. Usually, the d-axis of the reference frame is defined in the direction of the stator flux space vector which can be estimated from the measured stator voltage and current. The q-axis leads the d-axis by 90°. Given the amplitude of the stator flux linkage, the rotor current component in the q-axis is approximately proportional to the air-gap torque developed in the machine while the d-axis current component determines the reactive power measured on the stator side. By means of the d- and q-axis voltages, which can be provided by the rotor side PWM converter, decoupled control of the torque and reactive power can practically be achieved. The controller of a grid-connected DFIG is shown in Fig. 2. For a DFIG connected to the grid, as its torque and reactive power are related to real power and terminal voltage, other combinations of control variables exist to fulfill the requirements of power system dispatching [11].

At the front end of the controller shown in Fig. 2, the q-axis current demand is obtained from a quadratic relationship between the desired torque and the rotor speed, which is used as an input signal. This is consistent with the cubic relationship between the power and speed for optimal power tracking as mentioned earlier. The current demand in the d-axis is usually determined by an outer control loop attempting to regulate the terminal voltage of or the reactive power produced by the machine. Proportional and integral (PI) control is used in both axes to derive the reference voltage for the converter. The rotor current components (i.e., the feedback in the control loops) are calculated using the measured phase quantities i_{r_abc} projected to the d- and q-axes taking into account the rotor angle θ_r. The compensation terms for the voltages on the d- and q-axes are to decouple the current response in the two axes, and details of these terms can be found in [9] and [12].

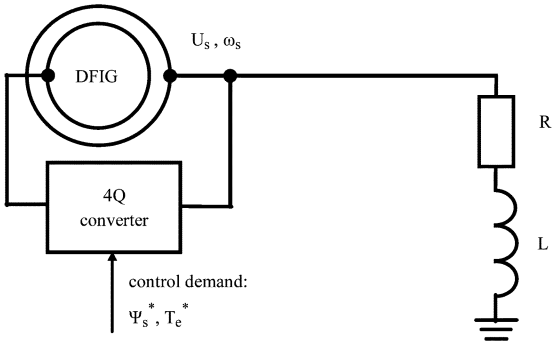

Fig. 3. DFIG in islanded operating mode.

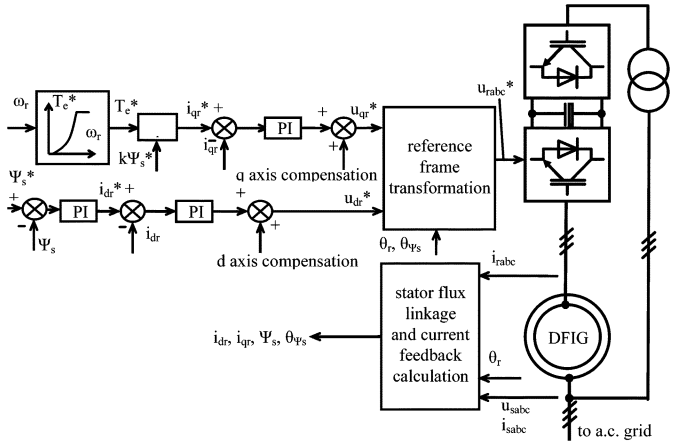

Fig. 4. Modified controller for a DFIG in islanded operation.

In the above controller, the stator flux linkage is decided to a large extent by the stator voltage which, in many cases, is almost fixed by the relatively strong grid. If DFIGs are connected to an HVdc rectifier station without a stiff ac voltage source, this is similar to the case of a DFIG supplying a purely passive load, as illustrated in Fig. 3. The four-quadrant (4Q) converter consists of two PWM VSCs connected back to back and the coupling transformer as shown previously in Fig. 2. Although the grid-side converter could define an ac voltage source, it is normally required to follow the change of system frequency instead using, for example, a phase-locked loop (PLL).

The terminal voltage and frequency are both variables. They are, however, dependent on each other as approximated below

$$U_s = \sqrt{3}\psi_s\omega_s \tag{1}$$

where U_s represents the root-mean-square (rms) value of the line-line voltage and ψ_s is the rms flux linkage per stator phase. ω_s is the angular frequency. The stator resistive voltage drop has been ignored.

From the machine point of view, it is important to keep its flux at an appropriate level irrespective of the mode of operation. Since the frequency is variable and it affects the voltage in the islanded mode, it is now necessary to specify the reference stator flux linkage explicitly in the controller. The machine torque can then be controlled through the q-axis current. For a given stator flux linkage, the terminal voltage will be determined according to the frequency achieved during operation. As to be shown next, the frequency also depends on the load characteristic. With frequency at the nominal value, the voltage will also be roughly acceptable as long as the stator flux linkage reference given is appropriate. The modified controller, which specifies the stator flux linkage, is shown in Fig. 4. At a certain speed, the control targets are stator flux linkage and torque—the same as that shown in Fig. 2.

Assuming zero steady-state error in the above controller, the air-gap torque and the amplitude of the stator flux linkage of the generator will both be at their reference values. The output real power of the generator is then approximately equal to the product of the machine air-gap torque and the rotor speed ignoring the losses. Further, assume that the wind speed is known at a particular moment. According to the $T_e^* - \omega_r$ relationship for optimal power tracking, the output real power of the DFIG should also be known. This value is denoted as P_G. With the constraints of P_G and ψ_s, the stator voltage and frequency can be decided jointly with the load characteristics which are expressed in the following equations for a series R and L static load.

The real and reactive power of the load can be written in terms of the voltage and frequency, and are equal to the real and reactive power of the generator

$$P_G = \frac{U_s^2}{R^2 + (\omega_s L)^2} R \tag{2}$$

$$Q_G = \frac{U_s^2}{R^2 + (\omega_s L)^2} \omega_s L = \frac{\omega_s L}{R} P_G \tag{3}$$

where Q_G represents the generator reactive power.

Considering again the relationship between stator voltage and flux linkage [i.e., (1)], the frequency and voltage in the steady-state operation can be derived as below

$$\omega_s = \sqrt{\frac{P_G R^2}{3\psi_s^2 R - P_G L^2}} \tag{4}$$

$$U_s = \sqrt{\frac{3P_G R^2 \psi_s^2}{3\psi_s^2 R - P_G L^2}}. \tag{5}$$

It can therefore be concluded that the control characteristic of the DFIG and the power-voltage/frequency characteristic of the load will jointly determine the frequency and voltage of the system. The approach taken above can be directly applied to scenarios having multiple DFIGs in the islanded system because the frequency and voltage are common variables to all generators in parallel, taking into account their transformers, and the variables are still governed by (1). It is assumed that all machines are controlled in the same way to maintain the stator flux linkage constant. The effect of deviations of the flux reference between generators will be discussed later.

As the wind speed fluctuates, the output real power of the DFIG changes following the optimal power tracking control. As a consequence, the frequency and voltage will also change if the load condition remains the same. Fortunately, an HVdc link can quickly change the power extracted from the DFIGs. It is expected that this can be utilized and will contribute to the frequency and voltage control for the local system.

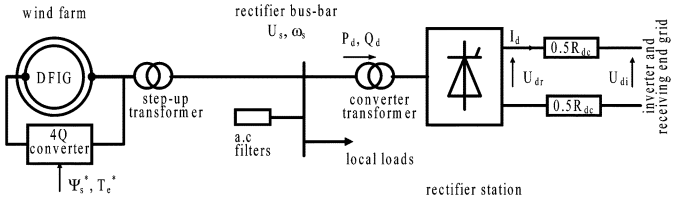

Fig. 5. Sending end model of an HVdc link.

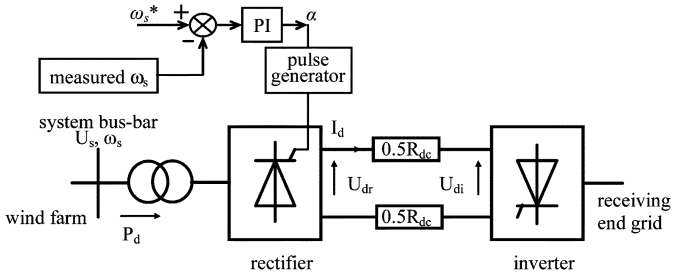

Fig. 6. Frequency control loop.

B. Control of HVdc Link

Consistent with the configuration of Figs. 1 and 5, the focus is now on the sending end of the HVdc link connecting the wind farm represented by a DFIG to the grid. In order to find the frequency and voltage at the local system busbar, it is useful to examine how the real and reactive power taken by the rectifier P_d and Q_d depends on the voltage and frequency. It is assumed that the ac filters are perfect so that the voltage waveform at the rectifier busbar is sinusoidal.

Referring to a typical monopole, 12-pulse arrangement for an HVdc link with metallic return, the quasi-steady-state equations relating to the ac- and dc-side variables are shown below in (6) [13], where L_c is the per phase leakage inductance of the converter transformer and R_c is the equivalent commutation resistance. R_{dc} is the total resistance of the dc transmission cable. The firing delay angle of the rectifier is denoted as α and the power factor angle as φ. It is assumed that the inverter of the HVdc link works on constant dc voltage control and that the voltage harmonics are ignored. This will simplify the analysis but the analysis and the derivation of the HVdc link control algorithm can be extended to other situations of the inverter system if required

$$\begin{cases} R_c = 2 \times \frac{3}{\pi}\omega_s L_c \\ U_{dr} = 2 \times 1.35 U_s \cos\alpha - I_d R_c \\ P_d = U_d I_d \\ Q_d = P_d \tan\varphi \\ \varphi = \cos^{-1}\left(\frac{U_{dr}}{2\times 1.35 U_s \cos\alpha}\right) \\ I_d = \frac{2\times 1.35 U_s \cos\alpha - U_{di}}{R_c + R_{dc}}. \end{cases} \tag{6}$$

At any moment, the real power to be taken away by the HVdc link is the difference between the output real power of the generators and the local loads plus losses. For a given P_d, a relationship can be established between the firing delay angle, the local system frequency, and voltage. The relationship is expressed below in (7), which is derived by substituting (1) into (6) followed by algebraic manipulation. It could be used to determine the firing delay angle needed to maintain the system frequency at the desired value

$$\begin{aligned} \cos\alpha &= f(\omega_s, \psi_s, P_d) \\ &= \frac{1}{R_{dc}\psi_s}\left[0.2042 \times L_c\left(\sqrt{U_{di}^2 + 4P_d R_{dc}} - U_{di}\right)\right. \\ &\quad \left. + 0.1069 \times R_{dc}\frac{\left(\sqrt{U_{di}^2 + 4P_d R_{dc}} + U_{di}\right)}{\omega_s}\right]. \end{aligned} \tag{7}$$

The left-hand side of (7), $\cos\alpha$, is dominated by the second term on the right-hand side, which implies that if the frequency is to be reduced, the firing delay angle should decrease; the firing instant would then advance. This can be understood from the operating characteristics of the generators and HVdc link. When the firing delay angle decreases, for the same dc voltage required at the sending end to maintain the power delivery, the ac-side voltage will be reduced. According to (1), the generator frequency will also reduce provided that the stator flux linkage is kept constant.

It should be pointed out that the above analysis did not involve generator speed information at all. Therefore, the result is generally valid for a wind farm of multiple DFIGs running at different speeds.

Equation (7) includes system and operational parameters which change during operation and are difficult to measure or estimate. It is therefore not practical to use the equation directly to determine the firing delay angle of the HVdc rectifier. Instead, based on the relationship illustrated by (7), it is possible to devise a negative feedback control loop for the system frequency as shown in Fig. 6 where ω_s^* is the reference angular frequency at the system busbar.

As an example, if the system frequency is too high, the controller will then decrease the firing delay angle. This seems to be similar to an HVdc link connecting a hydropower plant of synchronous generators to the grid, where a decreased firing angle means that more power is extracted by the HVdc link, slowing down the generators [14]. The present case is indeed conceptually different from any previously studied situations and the key of HVdc control is (1). The HVdc link is not controlling the real power. Instead, the real power is always determined by the DFIG power tracking algorithm and, of course, also the wind condition, which is independent of the system frequency and voltage to be regulated. Without energy storage in the sense of steady-state, the HVdc link must instantaneously deliver the generated power to the grid provided that the local loads are supplied. For a given firing delay angle of the HVdc rectifier, the system voltage and frequency will automatically be set to ensure the power balance. Therefore, no mechanical transient is involved in the frequency regulation process by changing the firing delay angle. This implies that the response of the regulation can be made very fast so that the frequency and voltage viewed by the local loads are almost constant. It is possible to add or switch off some DFIGs during operation. Starting of the wind farm and HVdc link can also be easily coordinated.

The reference for the stator flux linkage was assumed to be the same for all DFIGs in deriving (7). If it is appropriately set, the system voltage will be close to what is desired. In principle, a closed-loop controller can be designed to regulate the voltage by changing the reference of the stator flux linkage. In this study,

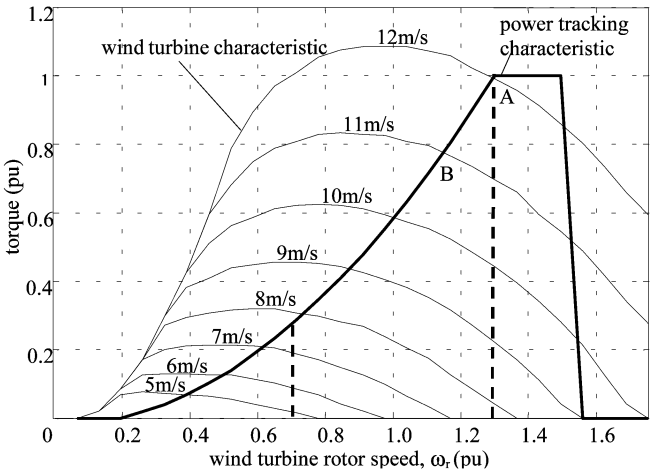

Fig. 7. Torque-speed characteristic.

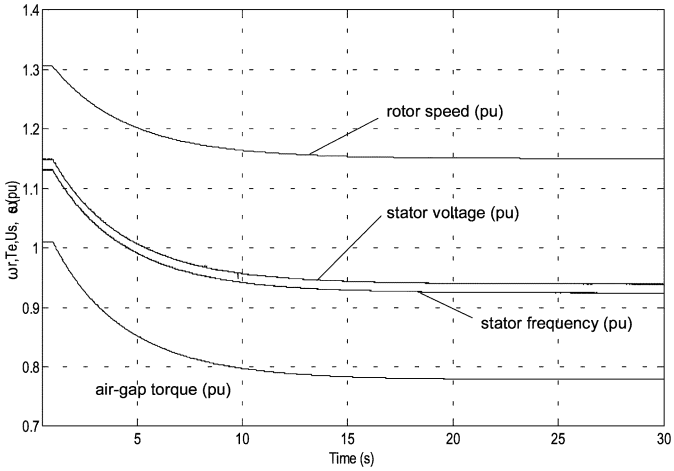

Fig. 8. Simulated response of DFIG in islanded operation-wind speed change.

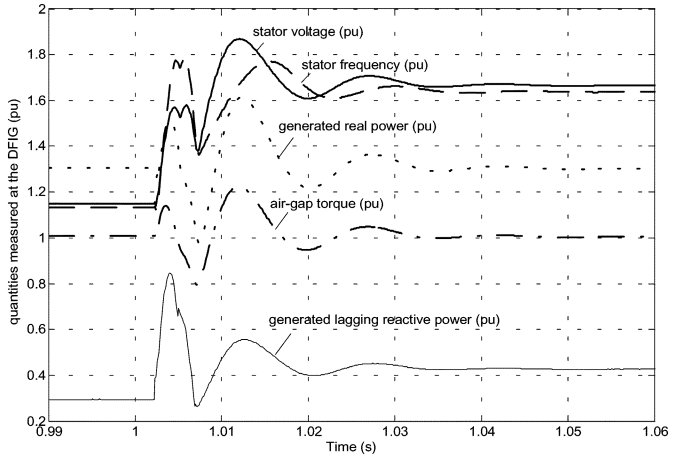

Fig. 9. Simulated response of DFIG in an islanded operation-load disturbance.

the reference flux is set and varied in discrete steps in order to approach the desired voltage amplitude. This is similar to setting the tap position in a transformer with an onload tap changer. While other strategies are also possible, the major advantage of the strategy adopted in the present study is to avoid the strong cross coupling between the frequency and voltage response of the DFIGs, which is likely to cause system instability.

In practice, the reference stator flux linkage can also be set differently for different machines. This will affect the reactive power from each generator. The difference between the reference values will eventually be absorbed by the leakage reactance of the step-up transformer associated with each DFIG unit. Although the DFIGs in an offshore wind farm are likely to be within a relatively small area, say 7 × 7 km [15], where the difference of wind speeds would be limited, it might be useful in some cases that some generators provide more reactive power during a specific period of time. This can be achieved by changing the stator flux linkage reference. From a practical point of view, it is desirable that all generators be controlled individually in an autonomous manner although some control demands may be issued to groups of generators collectively [16], [17].

III. Simulation Results

Simulations were performed in MATLAB/SIMULINK. The objective of simulation is to illustrate interacting phenomena which have not been understood before and verify the control strategy [i.e., (1) and Fig. 6] proposed in this study. In line with the above analyses, simulations were first performed on a DFIG in the islanded operating mode before being extended to include the HVdc link. Variation of the stator flux linkage reference of the DFIGs was also demonstrated with the HVdc link included.

A. DFIG in Islanded Operation

The system simulated is the same as shown previously in Fig. 3. A 2-MW DFIG supplies an RL load. Parameters of the generator are given in Appendix A. Simulations are carried out for two cases with changes of the wind input and load impedance, respectively.

The torque-speed characteristics of the wind turbine and generator are shown in Fig. 7. It is assumed that the turbine has been designed for a nominal wind speed of 12 m/s. The bold line represents the control trajectory of the DFIG which will normally operate in the speed range from 0.7 to 1.3 p.u. [4]. At a wind speed of 12 m/s, the input torque achieved is 1 p.u. All per-unit values are based on the generator (stator for power) ratings as given in Appendix A. The characteristic of the turbine is represented in Heier approximation [18], [19].

Suppose that the wind speed suddenly drops from 12 to 11 m/s. Following the change, the mechanical torque of the turbine will step from 1 p.u. down to about 0.77 p.u. because of the relatively high inertia the rotor tends to hold its speed. The unbalance between the mechanical torque and air-gap torque of DFIG leads to deceleration of the turbine. With effect of the DFIG air-gap torque control along the curve shown in Fig. 7, the wind turbine operation will eventually transit from point A to point B. As the exported real power declines, the stator frequency will reduce and so will the voltage amplitude. The simulation results are shown below in Fig. 8. Although the electrical transient is fast, it takes about 10 s for the whole system to enter a new steady-state due to the relatively long mechanical time constant.

The second case simulated is for a sudden change of load and the simulation results are shown in Fig. 9. The initial apparent load power is 1 p.u. with a lagging power factor of 0.98.

Half of the load is suddenly lost/shed with doubled R and L values in the load representation. The purpose of the simulation is to investigate the interaction between the DFIG and the isolated load, assuming an unrealistic scenario in which the generator controller is totally ignorant of the change of load. In this case, the real power generated by the DFIG remains the same and so does the machine stator flux linkage reference. The new steady-state values of the frequency and voltage amplitude can be determined using (4) and (5) based on the new R and L values of the load. It is clear that both frequency and voltage increase causing a load regulation effect which helps to re-establish power balance in the new steady-state. It is obvious that the transient process in this case is much faster than in the first case. This is because it is dominated by the electrical interaction in the system.

The HVdc link can be controlled to some extent to emulate the effects of load change on the DFIG in order to gain the control over the frequency and voltage of the local ac system. This is demonstrated next.

B. Wind Farm With HVdc Link

The system configuration is the same as previously shown in Fig. 1. The wind farm is simplified as an equivalent DFIG which represents the dynamics of 350 DFIGs, each rated at 2-MW stator power. The DFIG is assumed to be the same as that used above. The peak power extracted from the wind will be approximately 910 MW: 700 MW being produced from the stator side with the remaining 210 MW (i.e., 30%) of the stator power, being generated from the rotor side of the DFIGs at the maximum supersynchronous speed. Two stages of 50-Hz ac voltage transformation are used in the local ac system. There are 0.69 kV/30 kV and 30 kV/145 kV. The stepped-up voltage is then fed to the converter transformer which is specified for a 400-kV monopole 12-pulse HVdc link. The total reactive power rating of the ac filters is 240 MVAr (at 50 Hz) and the maximum power to be carried by the HVdc link is designed to be 770 MW, taking into account the local loads which are represented using resistance in series with inductance. At the nominal frequency and voltage, the local load has an apparent power of 150 MVA with a power factor of 0.9 lagging. Parameters of the HVdc link are detailed in Appendix B.

Although an aggregated model is used for the DFIGs in the wind farm, the controllers of the DFIGs and the HVdc link are independent in simulation and the later controller only measures the system bus frequency and voltage which are common to all DFIGs. This is therefore adequate to represent a wind farm of many DFIGs operating at different speeds.

Simulated scenarios are for sudden changes of wind speed and local loads. Supposing the wind speed is step increased from 11 to 12 m/s, the response is shown in three groups in Fig. 10. No local load is connected. The generator speed and air-gap torque both increase while the stator flux linkage is constant [Fig. 10(a)]. The real and reactive power from the generator increases as the changes of system frequency and voltage are largely constrained [Fig. 10(b)]. The constant local frequency and voltage are predominantly due to the control effect of the HVdc link, which adjusts the firing delay angle at the rectifier end according to the measured change of system frequency.

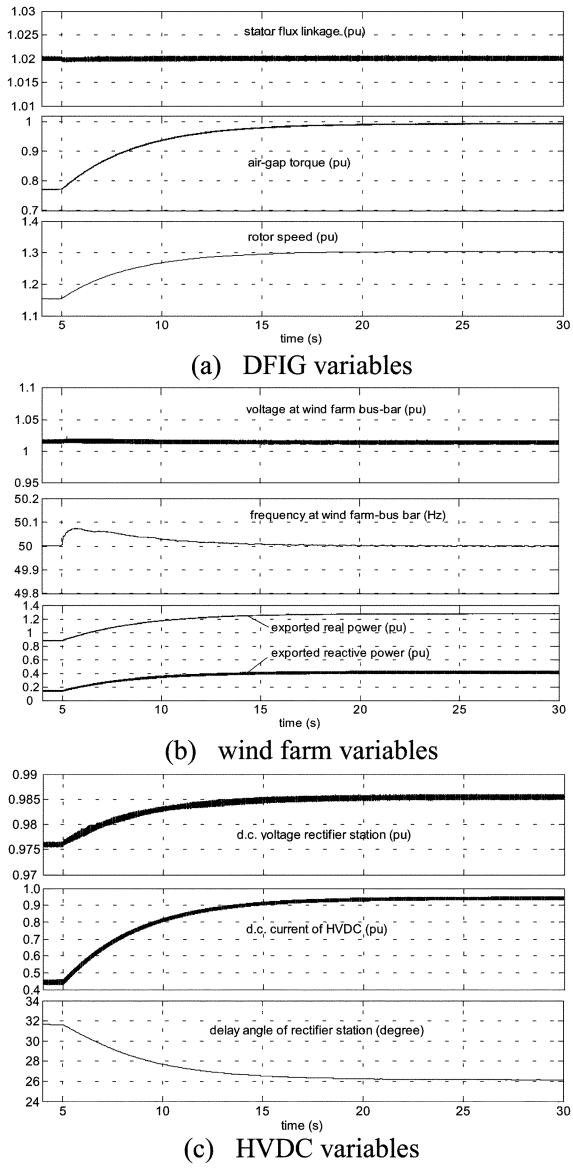

Fig. 10. Response of wind farm with an HVdc link—wind speed change.

While the increase of real power is caused by the increase of wind speed, the reactive power is increased because the HVdc converter station now needs more reactive power. From the generator point of view, the increased reactive power is provided by increasing the stator current component in the d-axis. This is further caused by the change of rotor current using the rotor-side converter in order to keep the stator flux linkage constant. The response of the HVdc link is shown in [Fig. 10(c)]. Reduction of the firing delay angle causes the rectifier dc-side voltage and, hence, the dc current to increase; therefore, more power is delivered.

The inverter side of the HVdc link is represented by a dc voltage source without harmonics. The harmonic signatures shown in the simulation results are therefore unrealistic. However, for the DFIG controller at the sending end, the harmonics present in the system voltage and current due to the HVdc link are modeled with reasonable accuracy and the purpose of the work is to examine interaction effects at the DFIG sending end, not the HVdc receiving end.

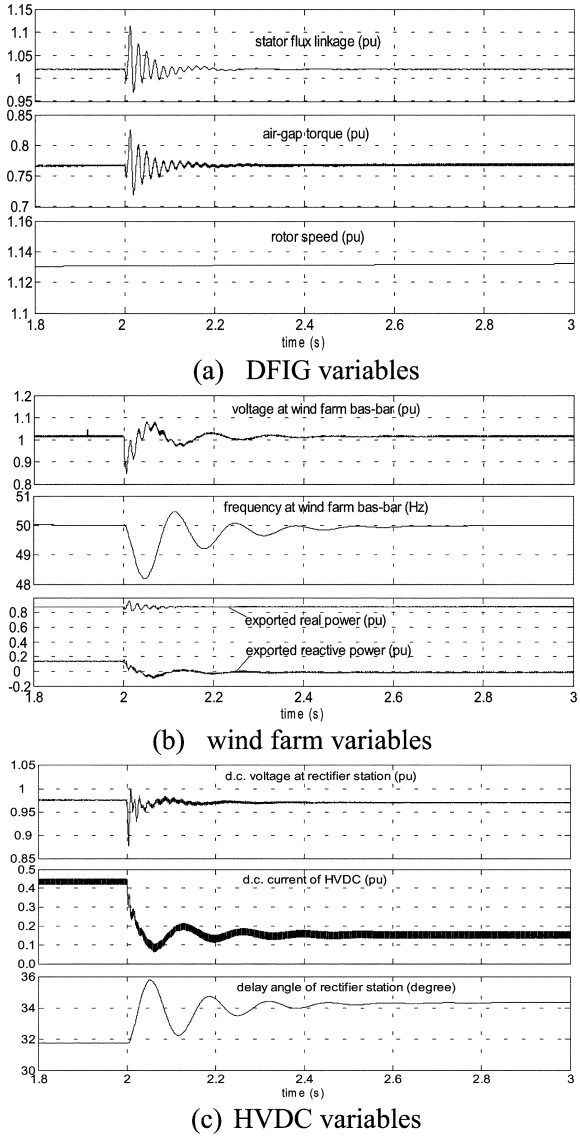

Fig. 11. Response of the wind farm with an HVdc link—local load disturbance.

Fig. 11 shows the response of the integrated system to a load disturbance. Again, the wind farm initially operates at a partial output corresponding to a wind speed of 11 m/s. The local loads are then applied. A fast electrical transient is excited, subject to the control actions of the DFIG and HVdc link. The operating state of the aggregated machine is eventually unchanged because the wind speed has not changed. The local loads initially cause a dip of system frequency and voltage which activates the HVdc controller. The firing delay angle at the rectifier end ramps up so that less power is delivered to the grid by the HVdc link while some of the generated power provides the local loads. In the new steady-state, which is reached in about 300 ms, the system frequency returns to its value prior to the load disturbance and the voltage returns to its prior value.

The main purpose of the simulations is to demonstrate the interactions between the different parts of the integrated system and the effects of the HVdc control. If, for example, the transient response of the system frequency and voltage is not acceptable from the local load point of view in practice, it is possible to tune the control gains of the HVdc link to improve the performance. Furthermore, a more sophisticated control algorithm can also be used instead of the PI algorithm to adjust the firing delay angle. This, along with more details of the interactions between multiple DFIGs with difference reference stator flux linkage, is beyond the scope of the present paper and will be addressed in the future.

C. Flexibility of Control

The main objective of this study is to investigate a control strategy that coordinates the control of the DFIGs and the HVdc link. In the proposed strategy, the DFIGs are controlled in almost the same way as if they were connected directly to an ac network. The only significant modification is to change the terminal voltage or reactive-power control into stator flux linkage control. As the stator flux linkage of the machine is estimated in standard DFIG vector control, the change can be readily implemented. The firing delay angle, not the power, of the HVdc link is adjusted according to the local system frequency. Although this may appear quite similar to the practice with HVdc links connected to synchronous generators, the underlining mechanism is very different. In the present case, the change of the firing delay angle does not necessarily mean a change in the power delivered by the HVdc link. The only purpose of changing the firing delay angle of the rectifier here is to control the frequency and, consequently, the voltage.

Control of the HVdc link can change the stator frequency and indirectly the terminal voltage which also depends on the stator flux linkage. Fig. 12 shows the simulation results as the stator flux linkage reference undergoes a step change. At $t = 2$ s, the reference changes from 1.02 to 1.1 p.u. Correspondingly, the system voltage increases while the frequency remains the same. The dc current decreases slightly, implying that the power delivered by the HVdc link is reduced. This is because the increase of the ac system bus voltage causes the local loads to absorb more power generated by the DFIGs. The simulation clearly shows that the stator flux linkage can be controlled as an independent variable to further adjust the voltage.

It is advisable that the stator flux linkage reference be changed in a discrete manner since the firing delay control of the rectifier in the HVdc link also affects the local system voltage. This helps to avoid control instability.

IV. Conclusion

This paper has investigated the control requirements when a wind farm of DFIGs is connected to the grid using a conventional thyristor-based HVdc link. A strategy of coordinated control for DFIGs and an HVdc link is proposed based on the understanding of the interactions between them. From the DFIG point of view, such control is achieved by providing a reference for the stator flux linkage instead of the terminal voltage or output reactive power. With this modification, the capability of optimal power tracking is retained with the DFIG. The firing delay angle of the rectifier at the sending end of the HVdc link can be used to regulate the frequency of the local ac system frequency and, hence, the voltage indirectly. The voltage can be further adjusted by the generator stator flux linkage reference.

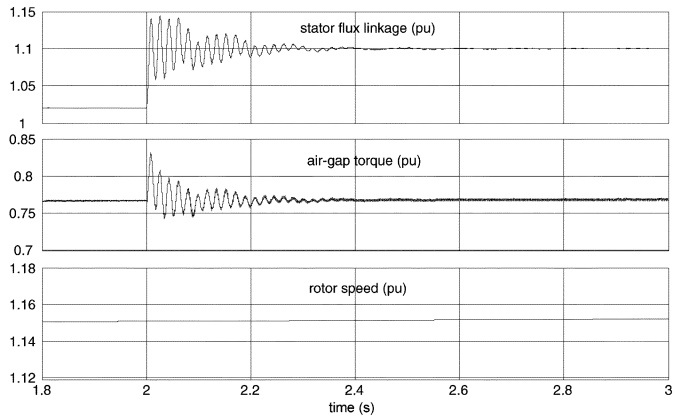

(a) DFIG variables

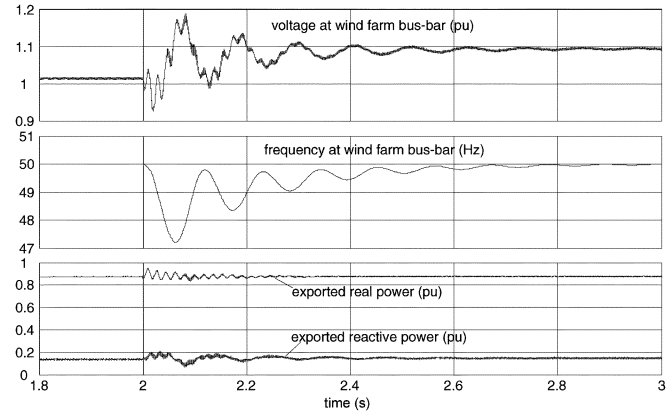

(b) wind farm variables

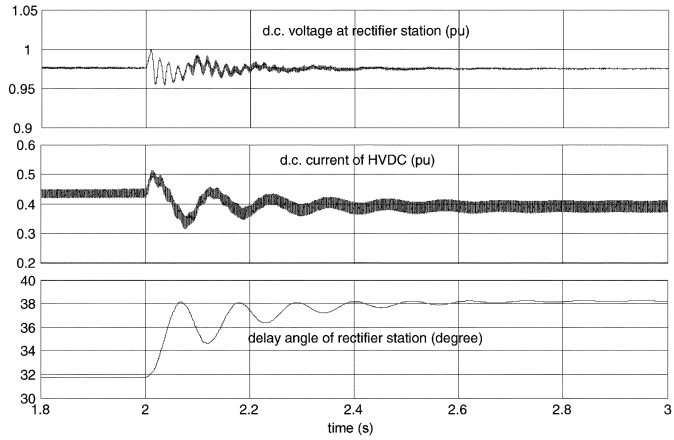

(c) HVDC variables

Fig. 12. Response of the wind farm with an HVdc link—change of reference stator flux linkage.

It is expected that the study will help wind turbine and HVdc system manufacturers, as well as wind farm developers, to recognize the control requirements and devise appropriate control strategies for some potential applications.

APPENDIX A
PARAMETERS OF DFIG

Per-unit system of DFIG

base capacity $S_b = 2$ MW;
base frequency: $f_b = 50$ Hz;
base stator voltage (phase, peak value) $V_{sb} = 563.4$ V;
base stator current (peak value) $I_{sb} = 2.3667$ kA;
base impedance on stator side $Z_{sb} = 0.2381\ \Omega$;
base rotor voltage (phase, peak value) $V_{rb} = 897.18$ V;
base rotor current (peak value) $I_{rb} = 1.5218$ kA;
base impedance on rotor side $Z_{rb} = 0.5758\ \Omega$;
base stator flux linkage $\Psi_{sb} = 1.553$ V-s;
base torque $T_b = 12.732$ kNm;
base speed $n_{rb} = 1500$ r/min.

Parameters of DFIG (star equivalent circuit):

$S_n = 2.0$ MW, $f_n = 50$ Hz, $U_n = 690$ V (line–line, rms);
winding connection (stator/rotor): star/star;
number of pole pair $P_p = 2$;
turn ratio $N_s/N_r = 0.643$;
stator resistance $R_s = 0.098\ 41$ p.u.;
stator leakage inductance $L_{ls} = 0.1248$ p.u.;
rotor resistance $R_r = 0.005\ 49$ p.u.;
rotor leakage inductance: $L_{lr} = 0.099\ 55$ p.u.;
magnetizing inductance: $L_m = 3.9527$ p.u.

APPENDIX B
PARAMETERS OF HVdc LINK

Per-unit system of HVdc

base dc voltage 400 kV;
base dc current 1925 A;
base capacity 770 MW.

Parameters of ac filters

Four single-tuned filters for 11th, 13th, 23rd, and 25th harmonics each with 60-MVAr-rated capacitive reactive power at 50 Hz.

Parameters of converter transformers

two converter transformers in Y-Y and Y-Δ;
rating 450 MVA;
transformer ratio 145/160 kV;
short-circuit impedance $0.0025 + j0.24$ p.u.

Parameters of 150-km dc transmission line

resistance of per kilometer 0.0217 Ω/km;
inductance of per kilometer 0.792 $\mathrm{mH/km}$km.

Inductance of smoothing reactor 0.3438 H.

ACKNOWLEDGMENT

Dr. L. Ran would like to thank Prof. K. Abbott of AREVA T&D, Stafford, U.K., for advice and helpful discussions.

REFERENCES

[1] S. Muller, M. Deicke, and R. W. De Doncker, "Doubly fed induction generator systems for wind turbine," *IEEE Ind. Appl. Mag.*, vol. 8, no. 3, pp. 26–33, May/Jun. 2002.
[2] W. Lu and B. T. Ooi, "Optimal acquisition and aggregation of offshore wind power by multiterminal voltage-source HVDC," *IEEE Trans. Power Del.*, vol. 18, no. 1, pp. 201–206, Jan. 2003.
[3] E. Spooner, P. Gordon, J. R. Bumby, and C. D. French, "Lightweight ironless-stator PM generators for direct drive wind turbines," *Proc. Inst. Elect. Eng., Electr. Power Appl.*, vol. 152, no. 1, pp. 17–26, 2005.
[4] B. M. Weedy and B. J. Cory, *Electric Power Systems*, 4th ed. New York: Wiley, 1998, pp. 141–141.

[5] L. Tang and B. T. Ooi, "Protection of VSC-multi-terminal HVDC against dc faults," in *Proc. IEEE Power Electronics Specialists Conf.*, vol. 2, Cairns, Australia, Jun. 2002, pp. 719–724.
[6] U. Axelsson, A. Holm, C. Liljegren, K. Eriksson, and L. Weimers, "Gotland HVDC light transmission—world's first commercial small scale dc transmission," in *CIRED Conf.*, Nice, France, May 1999.
[7] T. Thiringer, "Integration of large sea-based wind parks-how much power electronic devices are needed in order to avoid power quality problems on the grid?," in *Proc. IEEE Power Engineering Soc. Summer Meeting*, vol. 2, Chicago, IL, Jul. 2002, pp. 1277–1279.
[8] J. B. Ekanayake, L. Holdsworth, X. G. Wu, and N. Jenkins, "Dynamic modeling of doubly fed induction generator wind turbines," *IEEE Trans. Power Syst.*, vol. 18, no. 2, pp. 803–809, Apr. 2003.
[9] R. Pena, J. Clare, and G. Asher, "Doubly fed induction generator using back-to-back converters and its application to variable-speed wind-energy generation," *Proc. Inst. Elect. Eng., Electr. Power Appl.*, vol. 143, no. 3, pp. 231–241, 1996.
[10] B. Hopfensperger, D. J. Atkinson, and R. A. Lakin, "Stator-flux-oriented control of a doubly-fed induction machine with and without position encoder," *Proc. Inst. Elect. Eng., Electr. Power Appl.*, vol. 147, no. 4, pp. 241–250, 2000.
[11] Z. Krzeminski, "Control systems of doubly fed induction machine based on multi-scalar model," in *Proc. 11th World Congress International Federation Automatic Control*. New York, 1991, pp. 521–526.
[12] R. Pena, J. Clare, and G. Asher, "A doubly fed induction generator using back-to-back PWM converters supplying an isolated load from a variable speed wind turbine," *Proc. Inst. Elect. Eng., Electr. Power Appl.*, vol. 143, no. 5, pp. 380–387, 1996.
[13] J. Arrillaga, *High Voltage Direct Current Transmission*, ser. IEE Power and Energy Series 29. London, U.K.: IEE, 1998, pp. 10–55.
[14] P. Kundur, *Power System Stability and Control*. New York: McGraw-Hill, 1994, pp. 500–524.
[15] N. M. Kirby, L. Xu, M. Luckett, and W. Siepmann, "HVDC transmission for large offshore wind farms," *Inst. Elect. Eng. Power Eng. J.*, vol. 16, no. 3, pp. 135–141, 2002.
[16] J. L. Dallachy and I. Tait, "Guidance note for the connection of wind farms," in *SP Transmission and Distribution*. Perth, U.K.: Scottish Hydro-Electric, 2002.
[17] D. Xiang, L. Ran, P. J. Tavner, and J. R. Bumby, "Control of a doubly fed induction generator to ride through a grid fault," in *Proc. Int. Conf. Electric Machines (ICEM)*, Cracow, Poland, 2004.
[18] J. G. Slootweg, H. Polinder, and W. L. Kling, "Dynamic modeling of a wind turbine with doubly fed induction generator," in *Proc. IEEE Power Eng. Soc. Summer Meeting*, Vancouver, BC, Canada, 2001, pp. 644–649.
[19] L. Ran, J. R. Bumby, and P. J. Tavner, "Use of turbine inertia for power smoothing of wind turbines with a DFIG," in *Proc. IEEE Int. Conf. Harmonics Quality Power (ICHQP)*, Lake Placid, NY, 2004.

Dawei Xiang was born in Sichuan, China. He received the B.Eng. and M.Sc. degrees in electrical machinery and apparatus from the School of Electrical Engineering, Chongqing University, Chongqing, China, in 1999 and 2000, respectively.

Currently, he is a Lecturer of Electrical Machinery and Apparatus with Chongqing University. In 2004, he was a Visiting Scholar with Durham University, Durham, U.K. From 1999 to 2000, he was an exchange M.Sc. student with the University of Electro-Communications, Tokyo, Japan. His research interests include the control of doubly fed electrical machines as used in renewable energy systems.

Li Ran (M'98) received the Ph.D. degree in power systems engineering from Chongqing University, Chongqing, China, in 1989.

Currently, he is a Lecturer in Electrical Power and Control in the School of Engineering, University of Durham, Durham, U.K. He participated in the commissioning of the Gezhouba-Shanghai HVdc system in China in 1989. His research interests include the application of power electronics in power systems and renewable energy systems, such as wave and wind energy converters.

Dr. Ran received the Stanley Gray Award-Offshore Technology in 1999 from the Institute of Marine Engineers, London, U.K., for his study on the interconnection of offshore oil rigs.

Jim R. Bumby received the M.Eng. and Ph.D. degrees in engineering from the University of Durham, Durham, U.K., in 1970 and 1974, respectively.

Currently, he is a Reader in the Electrical Engineering Department in the School of Engineering, University of Durham, Durham, U.K. His research interests are in electrical power and control and novel generator topologies for new and renewable energy systems. He is also interested in hybrid electric vehicles.

Dr. Bumby received an IEE Power Division Premium in 1997 for work on direct drive permanent magnet generators for wind turbines.

Peter J. Tavner received the M.A. degree in engineering sciences from Cambridge University, Cambridge, U.K. in 1969 and the Ph.D. degree from Southampton University, Southampton, U.K., in 1978.

Currently, he is Professor of New and Renewable Energy in the School of Engineering, University of Durham, Durham, U.K. He has held a number of research and technical positions in industry including Technical Director of Laurence, Scott & Electromotors Ltd., Norfolk, U.K. and Brush Electrical Machines Ltd., Loughborough, U.K. Most recently, he has been Group Technical Director of FKI Energy Technology, Loughborough. His research interests include electrical machines for the extraction of energy from renewable sources and their connection to electricity systems. He retains a particular interest in electromagnetic analysis, the application of condition monitoring to electrical systems, and the use of converters with electrical machines.

Dr. Tavner is a winner of the Institution Premium of the IEE.

Shunchang Yang was born in Shanghai, China. He graduated from the Electrical Engineering Department of Chongqing University, Chongqing, China, in 1960.

Currently, he is a Professor in the School of Electrical Engineering, Chongqing University. He was an Assistant Lecturer with Chongqing University, in 1960. From 1985 to 1986, he was a Visiting Scholar with the University of Tennessee, Knoxville. In 1991, he was with the Kiev Institute of Technology, Kiev, Ukraine, and the All Soviet Union Institute of Electrical Engineering and Sciences, Moscow, Russia, in an international project Asynchronized Synchronous Machines and their Applications in Power Systems. His research interests include the design and control of electrical machines of new topologies.